A Rheometrical Technique to Study the Swelling Kinetics of Vulcanized Rubber Particles by Paraffinic Solvents Using a Torque Rheometer

Vincent Gaulliard, Jean L. Leblanc

University P.&M. Curie (Paris 6), Polymer Rheology and Processing, F-94408 Vitry-sur-Seine, France

Received 28 April 2003; accepted 16 April 2004
DOI 10.1002/app.20791
Published online in Wiley InterScience (www.interscience.wiley.com).

ABSTRACT: The solvent uptake by vulcanized rubber particles was studied through a swelling technique by using a torque rheometer to record torque versus time curves, with good repeatability. Several experiments were performed to study the effects of varying the solvent/rubber ratio, the solvent type, and the rubber nature. The effects of the materials alone were also studied. A four-parameter mathematical model was developed, with a physical significance assigned to each of the parameters, and was compared with experiments. The model was found to fit well with the experimental results, therefore, allowing the physical processes involved in the solvent swelling of rubber particles to be investigated through model parameters. © 2004 Wiley Periodicals, Inc. J Appl Polym Sci 94: 142–153, 2004

Key words: ground tire rubber; paraffin hydrocarbons; torque rheometer; kinetics; swelling

INTRODUCTION

The problem of waste disposal management is a worldwide issue. Among all the waste polymer materials, the reuse of waste rubber coming from worn tires is even more complicated because of a crosslinked structure and a very long time period for natural degradation.

As land-filling of discarded tires is no longer permitted and their use as an energy source in cement factories and power stations is challenged by other waste materials, reclaiming scrap rubber appears the most desirable approach to solve the problem.[1] Therefore, whole tires can be shredded to produce ground rubber of a desired particle size. There are thus growing quantities of ground rubber particles that can nowadays be considered as raw materials for new applications. Considerable work has already been done in this area.[2–8] A number of potentially interesting processes involve the modification of ground particles by low molecular weight materials that have the capability of permeating vulcanized rubber and, therefore, to swell the particles, for instance, as a preliminary treatment before further chemical modifications.[9–10]

Swelling at equilibrium was used extensively to study crosslinked networks, but relatively little work was done to obtain complete swelling–time curves. The conventional gravimetric method at equilibrium swelling is the most common one but others have been suggested.[11–12]

In this article, a swelling technique is described that uses the torque rheometer, a well-spread instrument in most polymer laboratories.[13] Rubber particles of various origins and different solvents were used to develop an experimental protocol for reproducible torque curves. Then, various experimental parameters were systematically investigated, such as solvent/particles ratio, solvent type, nature of the rubber, etc.

Torque versus time curves show that, in the dynamic conditions of the experiments, several concomitant events take place that can be modeled by using a relatively simple approach. The significance of model parameters was sought, as a manner to understand the likely physical processes involved in the solvent uptake by rubber particles.

EXPERIMENTAL

Materials

Ground rubber particles, from passenger car and truck tires, were obtained from an industrial plant [Alliance Environnement, Oise (60), France], in which wholes tires were crushed at room temperature to produce fragments that are separated from steel wire, textile, and other contaminants. After several sieving and screening steps, 1- to 2-mm ground particles were obtained which exhibit the average composition given in Table I.

Correspondence to: J. L. Leblanc (jleblanc@ccr.jussieu.fr).

TABLE I
Average Compositions of Ground Rubber Particles

Material	Car tire particles	Truck tire particles
Rubber/Elastomers	60	60
Carbon black and silica	28	30
ZnO	1	2
Sulphur	1	1
Additives	10	7

A calorimetric analysis performed on both lots of materials shows that, as expected, truck tire particles consist of (filled) natural rubber (NR), whereas passenger car tire particles contain styrene–butadiene rubber (SBR) and polybutadiene (BR). Four different paraffinic solvents were used. Their main characteristics are summarized in Table II.

Test methods

Weighed quantities of rubber particles with measured volume of solvents were introduced in the cavity of a 300-mL Haake laboratory mixer fixed with Z-blade counter-rotating rotors. Rotational rate was 20 rpm; temperature was set at 20°C, and a dead load of 5 kg was used to maintain the cavity closed after ingredients were introduced. The chamber closing ram was modified in such a manner that liquids can be introduced when the cavity is closed. The experiments consisted of recording the measured torque versus time, as data files that were subsequently handled with the appropriate calculation software.

RESULTS

Observations

As shown in Figure 1, all torque–time curves exhibit a sigmoid shape, with an inflection point. Torque readings can be regarded as an indirect measurement of rubber particle swelling behavior. Indeed, as particles absorb solvent, they grow in size, which results in an increased resistance to blade rotation and hence a higher torque. A number of additional experiments were made by changing the blade rotational rate in the 10–100 rpm range. It was observed that the higher the rotational rate, the higher the torque but the sigmoid shape of recorded curves was essentially kept and plateau regimes were always eventually reached. It was therefore concluded that basic physical processes were marginally affected by rotational (or shear) rate, and 20 rpm was then selected as a standard condition for all the experiments reported here.

The diffusion theory for elastomers[15–16] is based on the assumption that the swelling starts through liquid absorption at the surface of the sample up to a certain concentration; then, swelling proceeds further by increasing the depth of the swollen layers.[17–20] Our results suggest considering the solvent uptake as a three-step sequence that confirms this view. First, rubber particles swell while some fluid remains that lubricates the flow into the mixer cavity. Then, the torque exhibits a sharper increase when enough solvent has been absorbed by rubber particles with the associated volume growth that further restricts blade rotation. Eventually, either all the solvent has been absorbed by rubber particles and hence their swelling stops or the swelling saturation is reached. In both cases, a torque plateau is reached.

With respect to the temperature of the experiments (20°C) and the boiling temperature of alcanes used (see Table II), no solvent evaporation occurs, as confirmed by experimental torque curves. Indeed, as seen in Figures 1(a, b) and 2, because the final plateau is reached for a given system in given conditions, it remains essentially flat for extended mixing time. This demonstrates that an equilibrium state is achieved, which we attribute to particle swelling saturation.

Other authors have already shown that sorption curves for solvent uptake as a function of the square root of time can exhibit a sigmoid shape at the beginning of the process.[21–23] Such features are commonly regarded as the signature for an anomalous or non-Fickian behavior. It can be found as a consequence of the presence of moving boundaries.[24–25] Such an effect is relevant in polymer networks that are well above their glass transition temperature. The swelling process can easily be considered through the concept of cooperative diffusion, because the network is less and less tight as swelling proceeds.

TABLE II
Characteristics of Solvents

	Chemical formula	Molecular weight (g/mol)	Molar volume (cm^3/mol)	Density	Hansen[14] solubility parameters at 25°C $(MPa)^{1/2}$	Boiling temperature (°C)
Decane	$C_{10}H_{22}$	142.29	195.9	0.730	15.8	174
Dodecane	$C_{12}H_{26}$	170.34	228.6	0.750	16.0	216
Tetradecane	$C_{14}H_{30}$	198.40	261.3	0.763	16.2	251
Hexadecane	$C_{16}H_{34}$	226.45	294.1	0.773	16.4	280

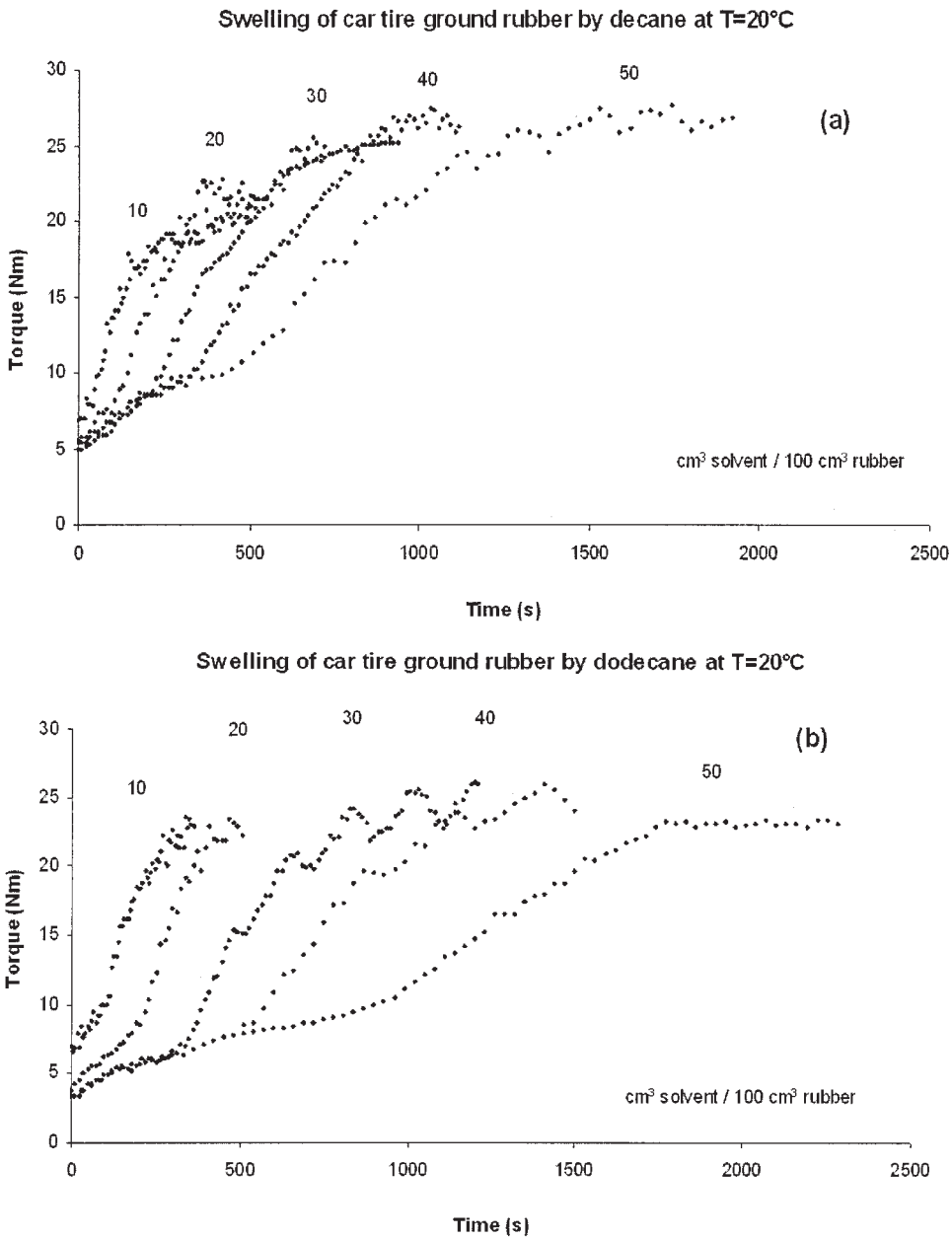

Figure 1 (a) Torque versus time curves; car tire particles; Decane. In running these experiments, a constant quantity ($V = 150$ mL) of rubber particles was introduced in the mixer; then the cavity was closed with the ram down with a load of 5 kg, before the selected quantity of solvent was injected in the mixing chamber. (b) Torque versus time curves; car tire particles; Dodecane, see (a). (c) Torque versus time curves; car tire particles; Tetradecane; see (a). (d) Torque versus time curves; car tire particles; Hexadecane; see (a).

Influence of solvent/particles ratio

As expected, the larger the solvent/rubber ratio, the longer the delay before the sharp increase is observed. The slope of the torque curve is also lowered with higher solvent ratio, which indicates slower swelling kinetics.

The initial torque depends on the solvent ratio and decreases toward a lower limit value while the solvent content increases, because lubrication is favored. The final torque increases with solvent quantity, as long as rubber can swell through solvent take-up. When particles are saturated, the maximum torque decreases slightly, which shows that some solvent remains outside rubber particles and lubricates the cavity.

Influence of solvent type

By comparing traces in Figure 1, the effect of the solvent nature is considered, all parameters being equal. Four paraffin hydrocarbons were chosen, with

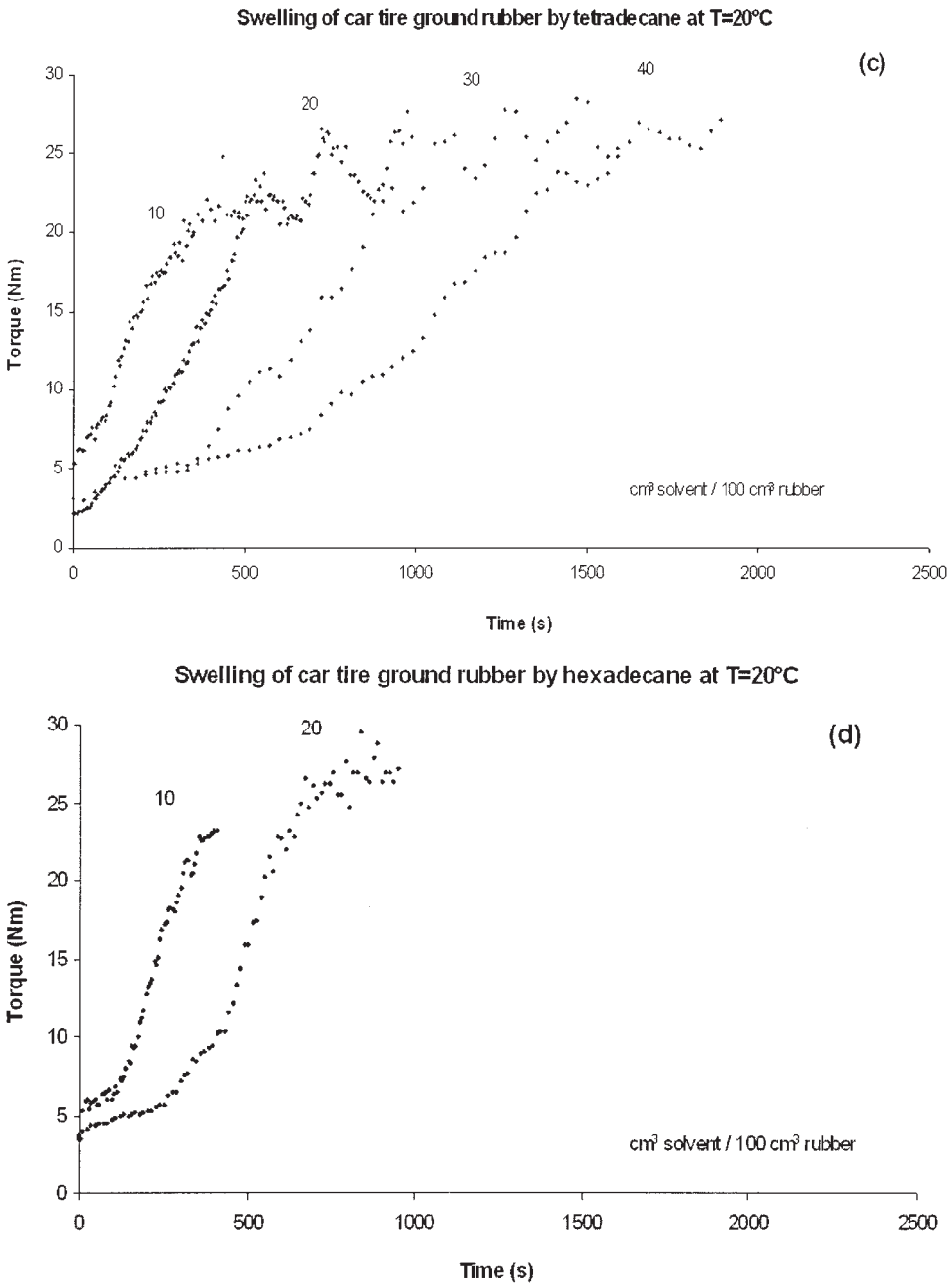

Figure 1 (*Continued*)

increasing chains lengths (from C_{10} to C_{16}), therefore with increasing molecular weight (MW), and all are liquids at $T = 20°C$. The torque curves show that the lower the solvent MW, the larger the uptake. Shorter times before the inflection point and lower values for the slope of the curves also indicate a faster swelling kinetic with these solvents. For the same volume of solvent, final torque values are about the same, whatever the solvent. Behavioral differences between solvents are significant with higher solvent/rubber ratios. The same observations are made either with car tire particles or with truck tire particles.

Influence of rubber nature

The influence of rubber nature is studied, all parameters being equal, by comparing results given by car tire particles on one hand and by truck tire particles on the other hand, with the same four solvents. Here, only results with dodecane are shown in Figure 2, which can be compared to Figure 1(b). Higher volumes of incorporated solvent indicate that the swelling is more important with NR. The kinetics of swelling is also faster with NR than with SBR, whatever the nature of the solvent. The higher torque values for the

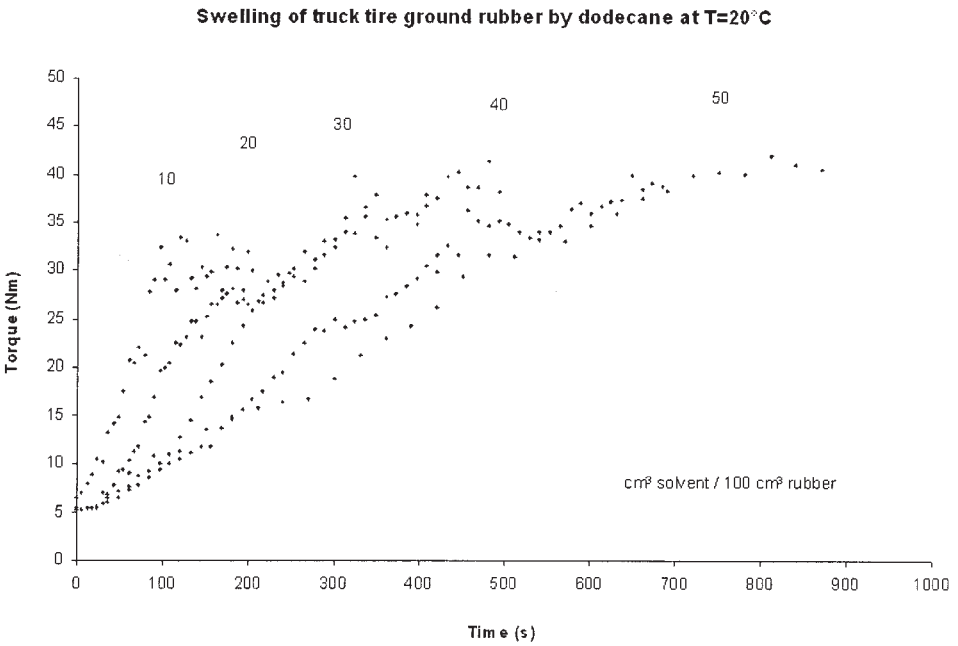

Figure 2 Torque versus time curves; truck tire particles; Dodecane; see legend to Figure 1 for experimental conditions.

same volume of solvent are only due to a geometrical aspect for the particles as discussed below.

MODELING

A mathematical model was developed for the torque curve with the objective to assign a physical meaning to all parameters. The following reasoning was therefore elaborated: at the beginning of the experiment, the mixer chamber is filled by two components: the solvent and the particles, whose fractions are, respectively, φ_{Solvent} and φ_{Part}, defined by:

$$\varphi_{\text{Solvent}} = \frac{V_{\text{Solvent}}}{V_{\text{Total}}} \quad \text{and} \quad \varphi_{\text{Part}} = \frac{V_{\text{Part}}}{V_{\text{Total}}} \quad \text{with}$$

$$V_{\text{Total}} = 300 \text{ cm}^3$$

Therefore, due to the solvent uptake, the fractions of each material vary with time, with respect to the equality $\varphi_{\text{Solvent}}(t) + \varphi_{\text{Part}}(t) = \text{constant}$.

Let us assume that the viscosity of the solvent (i.e., η_{solvent}) remains constant during the time of the experiment. Then, the torque Γ is a function of the values previously defined, for instance:

$$\Gamma = f[\varphi_{\text{Solvent}}(t), \eta_{\text{Solvent}}, \varphi_{\text{Part}}(t)] \tag{1}$$

The value of the measured torque is either affected by the solvent (at short times) or by the particles fraction in the rheometer (when the swelling is achieved), for instance:

$$\Gamma \propto \Gamma_{\text{Solvent}}(t) + \Gamma_{\text{Part}}(t) \tag{2}$$

and the two functions in the right member of the equation can be modeled with respect to experimental results.

Torque variation due to particles fraction, $\Gamma_{\text{Part}}(t)$, was investigated in a series of experiments whose results are given in Figure 3(a), in the case of car tire particles, and Figure 3(b) for truck tire particles. No solvent was used of course and all tests were made at fixed temperature (T = 20°C) and rotor speed (20 rpm). With the same volume of rubber, the higher torque value for truck tire particles is due to the geometry of the particles, which are roughly egg-shaped and less spherical than car tire particles, hence leading to a higher resistance to flow. The curves can be fit with the following mathematical function:

$$\Gamma_{\text{Part}}(t) = y_0 + a * \exp[b * \phi_{\text{Part}}(t)] \tag{3}$$

Parameters values for car tire particles and truck tire particles are given in Table III.

Another set of experiments was then performed to investigate the effect of the solvent fraction remaining outside rubber. Particle fraction was fixed at 0.5, and the torque value was taken before swelling could occur, to observe the effect of lubrication, for all the systems considered. As shown in Figure 4(a, b), solvents of high molecular weights show a higher lubrication effect, but a similar pattern is observed with respect to solvent fraction. Therefore, whatever the

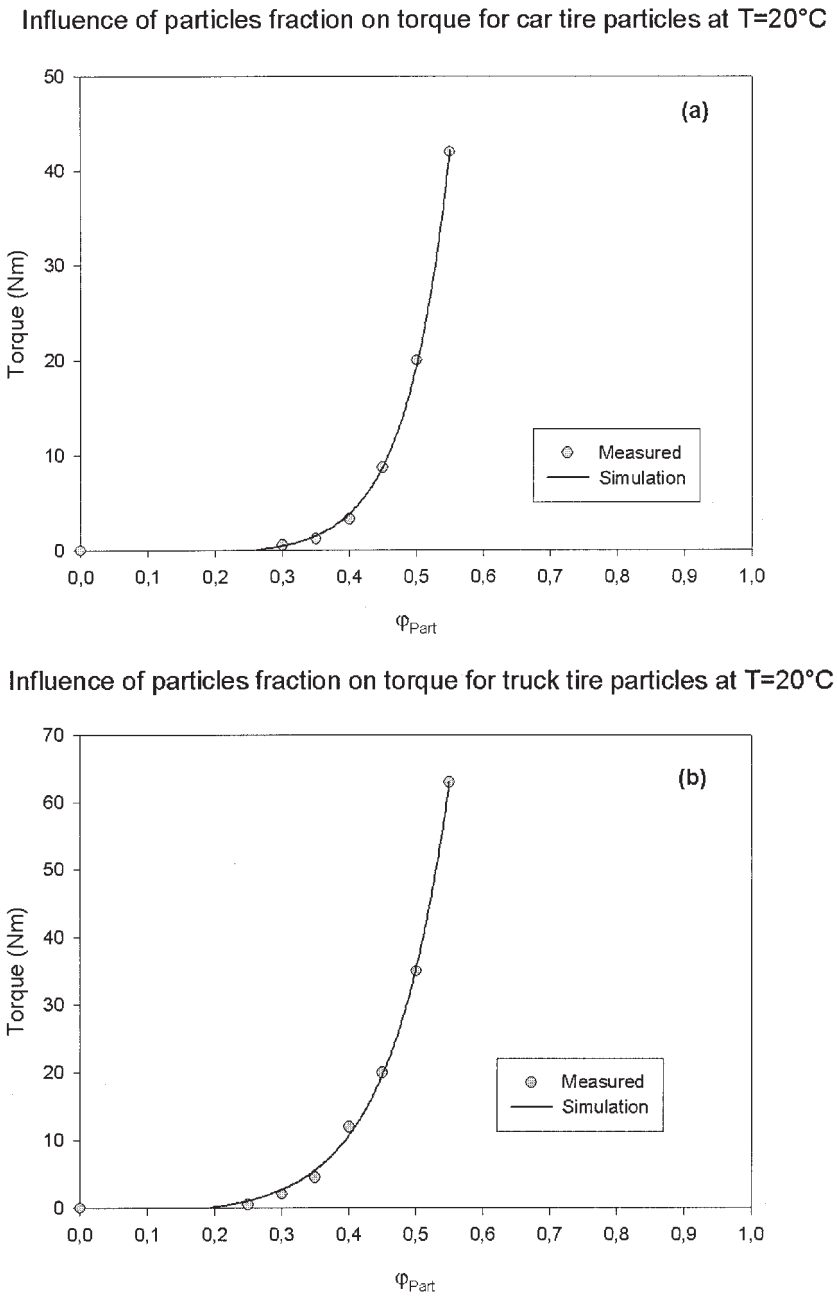

Figure 3 (a) Torque versus particle fraction; car tire particles. In running these experiments, only the selected quantity of rubber particles (no solvent added) was mixed in the closed chamber at 20°C until a stable torque was measured (usually within 60 s). (b) Torque versus particle fraction; truck tire particles; see (a).

system, the torque curves can be fit with the same kind of mathematical function, which is an important aspect for the modeling.

TABLE III
Expression of Γ_{Part} with Different Particles
$\Gamma_{Part} = y_0 + a \exp(b * \varphi_{Part})$

	y_0	a	b
Car tire particles	−0.52	0.0099	15.2
Truck tire particles	−1.13	0.1302	11.3

Equation (4) was then used to describe the rapid torque decrease with a small quantity of solvent:

$$\Gamma_{Solvent}(t) = (\Gamma_{Solvent})_\infty + [(\Gamma_{Solvent})_0 - (\Gamma_{Solvent})_\infty] * \exp[-c * \varphi_{Solvent}(t)] \quad (4)$$

Through nonlinear fitting, the parameters given in Table IV were obtained for all the systems investigated.

Results previously described [Figs. 1(a–d)] showed a rapid increase in the torque–time curves at the end

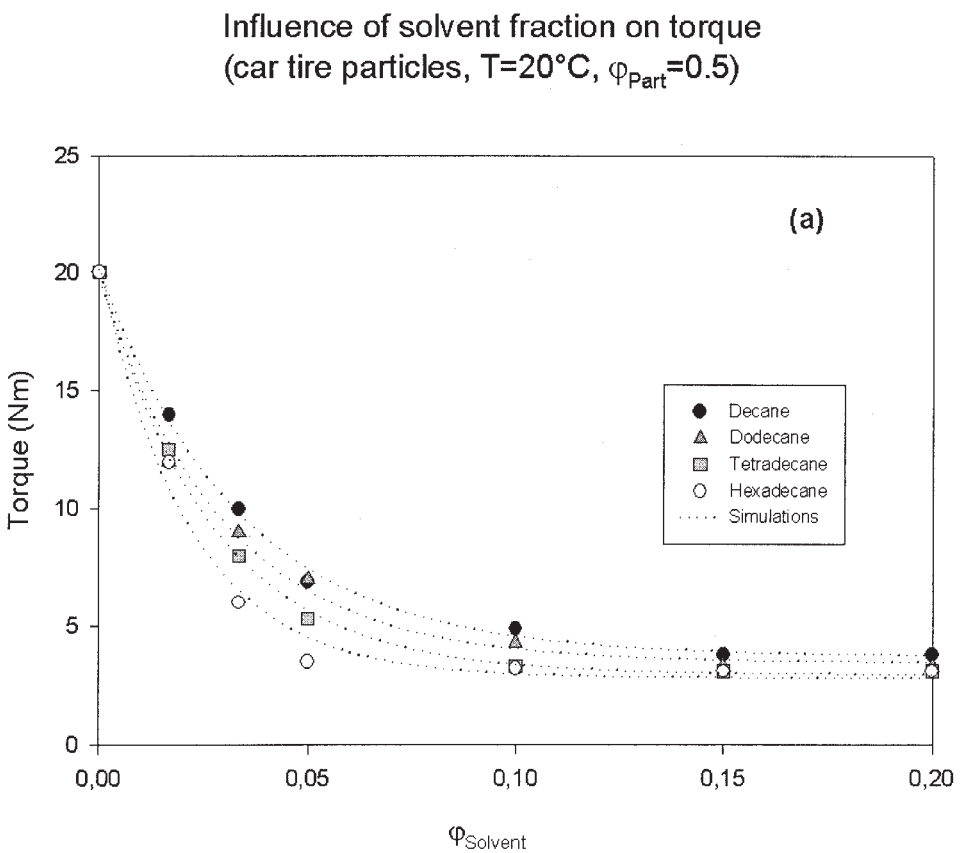

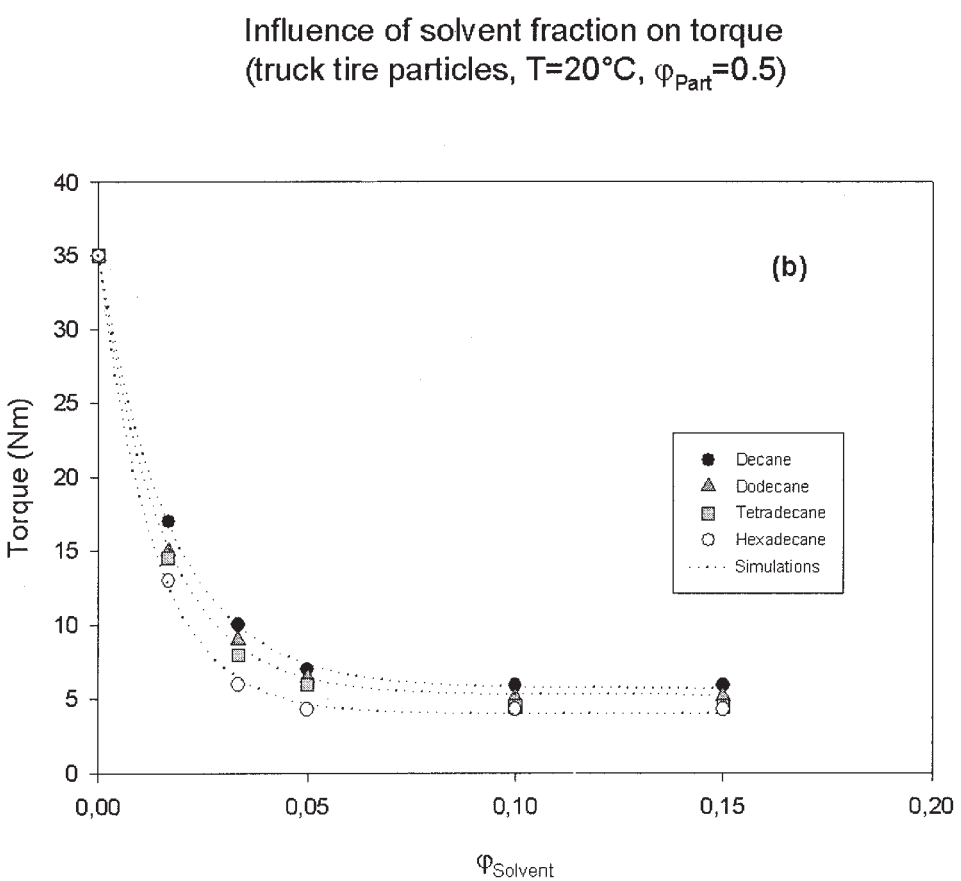

Figure 4 (a) Torque versus solvent fraction; car tire particles. In running these experiments, a fixed quantity of rubber particles (150 mL) was introduced in the mixer; then the chamber was closed with the ram down under 5 kg load and the appropriate quantities of solvent was injected. Torque value was immediately read as the experimental results reported in the figure. (b) Torque versus solvent fraction; truck tire particles; see (a) for experimental conditions.

TABLE IV
Expression of $\Gamma_{Solvent}$ with Different Solvents
$\Gamma_{Solvent} = (\Gamma_{Solvent})_\infty + [(\Gamma_{Solvent})_0 - (\Gamma_{Solvent})_\infty] * \exp[-c * \varphi_{Solvent}]$

	Car tire particles			Truck tire particles		
	Γ_∞	$\Gamma_0 - \Gamma_\infty$	c	Γ_∞	$\Gamma_0 - \Gamma_\infty$	c
Decane	3.72	16.4	29.6	5.74	29.3	58.0
Dodecane	3.46	16.3	33.5	5.29	29.7	65.4
Tetradecane	2.95	17.2	36.9	4.61	30.4	66.4
Hexadecane	2.69	17.6	45.7	4.02	31.0	76.6

of the swelling process. Consequently, the time to observe the inflection point can be used to draw the dependence of particle fraction on time (at this time t_0, $\varphi_{Solvent} = 0$ and φ_{Part} is determined by the initial conditions, i.e., by the initial quantities of solvent and rubber). This is an indirect method to document the swelling kinetics. Figure 5(a, b) suggests that, for a given solvent, the time to reach the inflection point in torque variation upon rubber particle swelling is varying from zero when $\varphi_{Part} = 0.5$ towards an infinite value $(\varphi_{Part})_\infty$ when the particle fraction reaches an asymptotic value that depends on the chemical nature of the solvent and of the rubber. Such expected observations correspond well to the fact that the ease of swelling is dependent on the chemical interaction between the rubber particles and the solvent. Decane is the lowest molecular weight solvent considered and is indeed giving rise to the shortest time to inflection point at constant φ_{Part}. Consequently, a suitable mathematical model to fit such experimental data would involve an exponential function, such as[26]:

$$\varphi_{Part}(t) = (\varphi_{Part})_0 + [(\varphi_{Part})_\infty - (\varphi_{Part})_0]*[1 - \exp(-Kt)] \quad (5)$$

where $(\varphi_{Part})_0 = 0.5$, $(\varphi_{Part})_\infty$ is the asymptotic value for an infinite time to inflection point, corresponding in fact to such a high level of solvent that, even for fully swollen particles, torque reading would remain essentially affected by lubrication effects, K is a rate parameter (in s^{-1}), and t is the time (s).

The product $K[(\varphi_{Part)\infty} - (\varphi_{Part})_0]$ expresses in fact how fast the solvent penetrates the rubber network and, with respect to eq. (5), one may expect higher absolute values of this product (because of the negative sign) for decreasing molecular weight of the solvent for a given rubber; these values for a given solvent are expected to be higher for truck tire particles. This is confirmed by results in Table V.

As can be seen in Figure 6, the asymptotic particle fraction $(\varphi_{Part})_\infty$ is decreasing with increasing molecular weight of the solvent; the chemical nature of the rubber particles also plays a role: as expected, NR-based particles exhibit a higher swell for a given solvent.

As a consequence to the expression of $\varphi_{Part}(t)$, the solvent fraction varies as follows:

$$\varphi_{Solvent}(t) = (\varphi_{Solvent})_0 - [(\varphi_{Solvent})_0 - (\varphi_{Solvent})_\infty] *[1 - \exp(-Kt)] \quad (6)$$

with the same constant K, which depends on the solvent and the rubber nature.

It follows that a mathematical model for the whole process can be proposed by considering balance between the effect of the solvent at shorter times and the effect of the particles fraction at longer times, through a function of the type:

$$\frac{1}{1 + \exp\left[-\frac{(t - t_0)}{s}\right]}$$

which is approximately equal to 0 for $t < t_0$ and 1 for $t > t_0$. With respect to eq. (2), the torque is then given by:

$$\Gamma \propto \left\{1 - \frac{1}{1 + \exp\left[-\frac{(t - t_0)}{s}\right]}\right\}\Gamma_{Solvent} + \left\{\frac{1}{1 + \exp\left[-\frac{[t - t_0)}{s}\right]}\right\}\Gamma_{Part} \quad (7)$$

When combining eqs. (3) and (5), and eqs. (4) and (6), quite a complicated relationship is obtained, but a simplification is easily made by weighing each parameter against others, to reduce their number to only four, essential to describe the experimental curves. These parameters are as follows: Γ_0 is the initial torque; G_∞ is the final torque; s is the slope of the curve; and t_0 is the inflection point time.

The above reasoning eventually leads to the following equation:

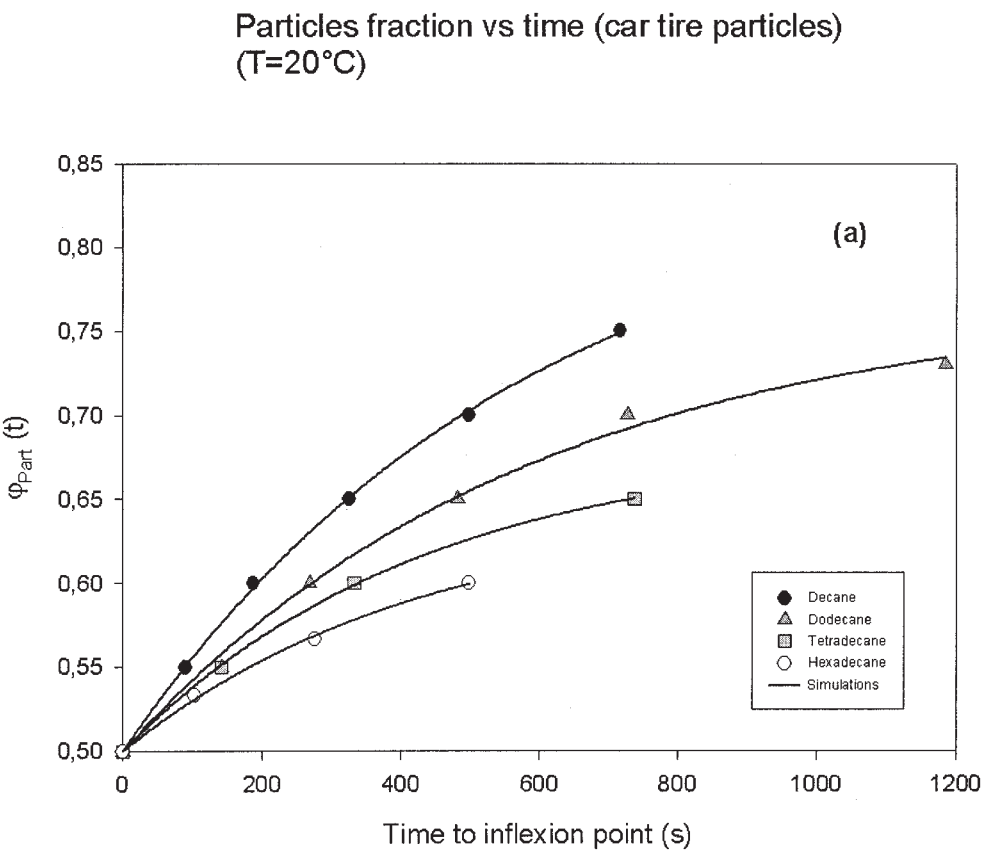

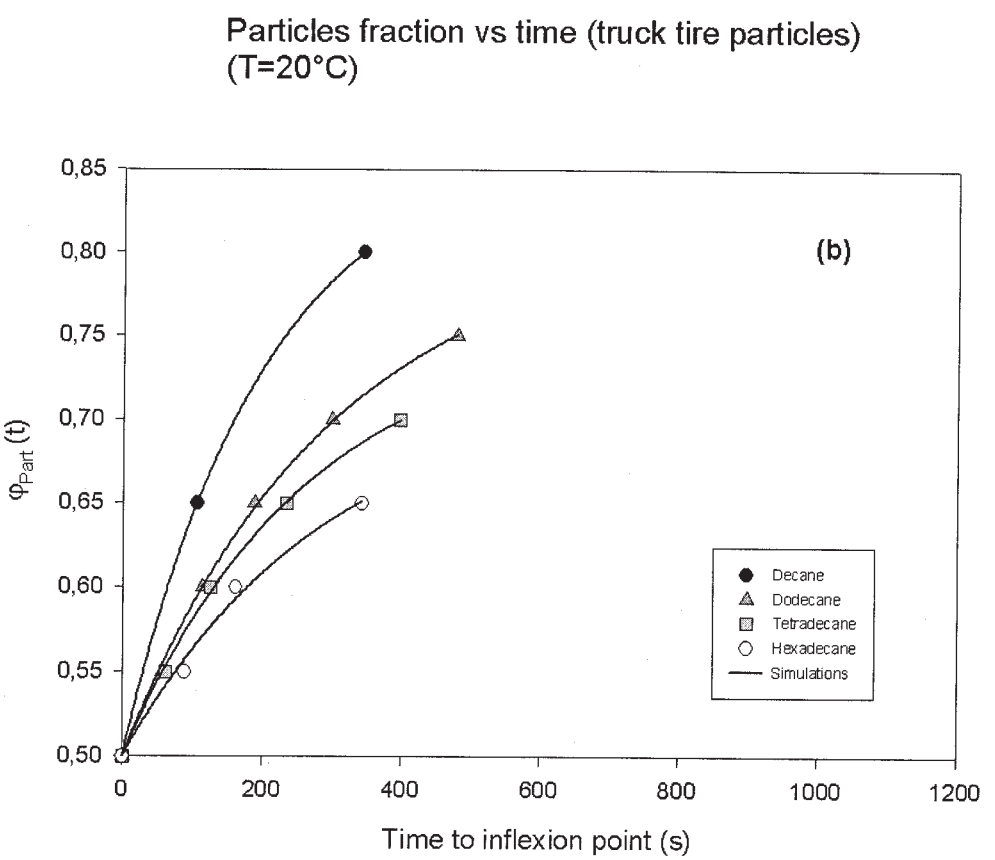

Figure 5 (a) Swelling kinetics; car tire particles. Data reported in this figure correspond to inflexion points read in Figure 1(a–d). (b) Swelling kinetics; truck tire particles. Data reported in this figure correspond to inflexion points observed in swelling experiments (e.g., Figure 2 in the case of dodecane).

TABLE V
Expression of $\varphi_{Part}(t)$ with Different Particles and Solvents
$\varphi_{Part}(t) = (\varphi_{Part})_0 + [(\varphi_{Part})_\infty - (\varphi_{Part})_0] * [1 - \exp(-Kt)]$, with $(\varphi_{Part})_0 = 0.5$

	Car tire particles			Truck tire particles		
	$[(\varphi_{Part})_\infty - (\varphi_{Part})_0]$	K	K* $[(\varphi_{Part})_\infty - (\varphi_{Part})_0] * 10^{-4}$	$[(\varphi_{Part})_\infty - (\varphi_{Part})_0]$	K	K* $[(\varphi_{Part})_\infty - (\varphi_{Part})_0] * 10^{-4}$
Decane	0.35	0.0017	5.95	0.37	0.0050	18.50
Dodecane	0.27	0.0017	4.59	0.31	0.0034	10.54
Tetradecane	0.18	0.0023	4.14	0.26	0.0038	9.88
Hexadecane	0.14	0.0024	3.36	0.22	0.0034	7.48

$$\Gamma = \Gamma_0 * \exp[1 - \exp(-Kt)] * \left\{1 - \frac{1}{1 + \exp\left[-\frac{(t - t_0)}{s}\right]}\right\} + \Gamma_\infty * \exp[-\exp(-Kt)] * \left\{\frac{1}{1 + \exp\left[-\frac{(t - t_0)}{s}\right]}\right\} \quad (8)$$

where K is the constant calculated in the solvent swelling kinetics and appearing in eqs. (5) and (6).

DISCUSSION

Results

Tables VI–VIII give the values of the four parameters of the model for some experimental conditions sufficient to discuss all the aspects of the physical process.

Influence of solvent/rubber ratio

The higher the solvent/rubber ratio, the higher the t_0 and s. The initial torque value Γ_0 is affected by the solvent content, because lubrication is not efficient at small percentages of solvent. The maximum value G_∞ slightly decreases with solvent content but the gap, $G_\infty - \Gamma_0$, increases with solvent content, because of a larger swelling.

One important aspect of our experimental results is that, at the end of rubber particles swelling, an equilibrium is reached in dynamic conditions. Indeed, while maintaining rotors rotation, torque curves remain essentially flat over extended periods. This demonstrates that, once the solvent has impregnated rubber particles, up to the maximum quantity permitted by the particular rubber network considered, no other physical process takes place, such as, for instance, squeezing out of solvent due to rotor shearing.

It is also worth underlining that any slippage effect of swollen particles (at the end of the swelling process) is de facto taken into consideration by the model, because the solvent/rubber ratio is a parameter.

Influence of solvent nature

The differences in swelling behavior between the four solvents are reflected by the values of the parameters.

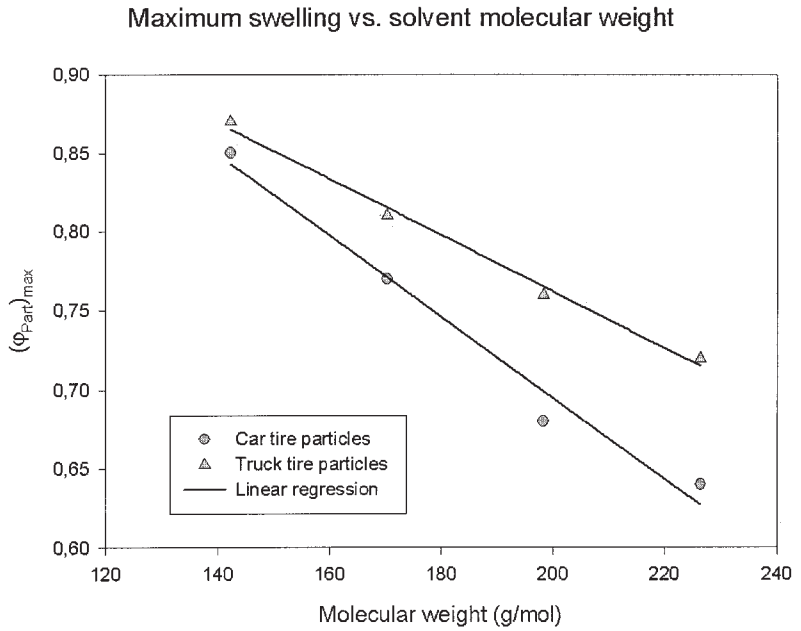

Figure 6 Maximum swelling versus molecular weight for all rubber nature considered.

TABLE VI
Model Results; Car Tire Rubber; Decane; $K = 0.0017$

cm^3 solvent/ 100 cm^3 rubber	10	20	30	40	50
Γ_0	7.0	5.5	4.8	4.3	6.0
Γ_∞	34.0	34.0	32.2	32.5	28.3
s	15.3	38.0	79.2	158.7	123.1
t_0	70.1	160.1	279.4	442.4	735.4

As can be seen, t_0 and s are smaller while decreasing the carbon chain length, which means a faster swelling kinetics. The initial torque value Γ_0 decreases while molecular weight increases because of a better lubrication. Associated, of course, with a slower solvent uptake by rubber particles, the gap $G_\infty - \Gamma_0$ does not significantly vary with the solvent, at a constant volume of solvent, which reflects quite similar values for the solvent–polymer interaction parameter for these systems. However, as can be seen in Figure 5, rubber particles can absorb larger amounts of low molecular weight solvent.

Influence of rubber nature

With NR-based particles, t_0 and s are smaller, reflecting a faster kinetics of swelling. The torque values, G_∞ and Γ_0, are larger with truck tire particles, but this is likely due to a geometrical effect, as commented earlier. By comparing Figure 5(a, b), it can be noted that NR-based particles are easier to swell and can accept a larger quantity of solvent, all others parameters being equal.

Effects of rubber particle shape and size distribution were also considered in separate experiments (not reported here). Essentially, it was observed that the smaller the particles, the faster the swelling kinetics, and the narrower the size distribution, the sharper the torque increase. Conversely, a wider particle size distribution gives a smoother torque increase, indicating that particles reach progressive saturation according to their sizes. Such results were expected from common sense reasoning and were considered as marginal with respect to our modeling approach.

TABLE VII
Model Results; Car Tire Rubber; Dodecane; $K = 0.0017$

cm^3 solvent/ 100 cm^3 rubber	10	20	30	40	50
Γ_0	7.0	4.8	3.8	4.0	4.2
Γ_∞	39.4	35.8	28.7	27.1	24.1
s	28.6	41.8	69.9	118.9	167.7
t_0	128.0	253.4	438.6	707.3	1264.9

TABLE VIII
Model Results; Truck Tire Rubber; Dodecane; $K = 0.0034$

cm^3 solvent/ 100 cm^3 rubber	10	20	30	40	50
Γ_0	7.2	5.5	4.6	4.3	6.1
Γ_∞	55.4	46.3	48.2	40.5	44.8
s	12.0	17.2	39.3	86.0	149.7
t_0	48.7	76.3	143.1	185.2	352.5

Comparing model and experiments

Equation (8) was used to fit experimental data, by using the nonlinear regression algorithm available in SigmaPlot® software (SPSS Science). For each curve, the four parameters (Γ_0, G_∞, s, and t_0) were obtained, while the K value was adapted to each solvent/rubber combination, to correspond to the physical process. As illustrated in Figure 7 with a few curves, good agreement between experimental and modeled curves is obtained.

It is worth underlining how the mathematical form of eq. (8) meets the complex physical processes involved in the experiments. Both the initial and the final torque levels, respectively, Γ_0 and G_∞ in eq. (8), are first affected by the particular swelling kinetics, essentially controlled by the constant K, which appears in the double exponential expression. Then, the sigmoidal torque uptake is expressed through the expression with an exponential in the denominator where the time t is the variable. The slope s and the inflection point time t_0 depend on the solvent/rubber ratio, as shown by the model parameters given in Tables VI–VIII. The model essentially assigns the same slope for the curves before and after the inflection point, but there is a large experimental scattering at low solvent percentage because the initial part of the curve is short. This has two consequences: at low solvent percentage, the model overestimates the final torque when compared to experiments, whereas at larger quantities of solvent, the model overestimates the initial torque, because the slope at short times is higher than the slope at long time in that case. This aspect confirms the view that, first, swelling is observed; then, when this process is completed, there is an expansion of the network until equilibrium is reached.

CONCLUSION

A simple rheometric technique to study the solvent swelling of vulcanized rubber particles under dynamic conditions was successfully developed and various experimental parameters were systematically investigated. Quite reproducible torque versus time curves were easily recorded with the appropriate ex-

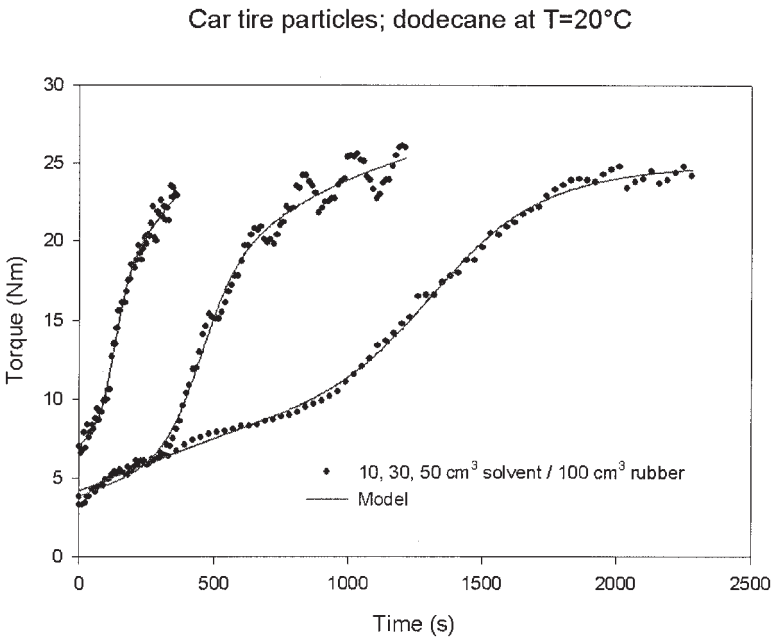

Figure 7 Comparison of model with experimental torque curves.

perimental procedure. A mathematical model, based on physical aspects of the experiment, was developed with only four parameters that fully account for the sigmoid shape of the torque curves. The model, shown to be in good agreement with experimental data, allows us to understand the physics involved in the process of solvent uptake by vulcanized rubber particles.

Such a rheometry-based technique could advantageously be used to study the compatibility of other polymers/fluids systems.

References

1. Adhikari, B. Prog Polym Sci 2000, 25, 909–948.
2. De, S. K.; Chakraborty, S. K.; Bhattacharya, A. K.; Phadke, A. A. Rubber Chem Technol 1983, 56, 726–736.
3. Pittolo, M.; Burford, R. P. Rubber Chem Technol 1985, 58, 97–106.
4. Klingensmith, B. Rubber World 1991, 203, 16–21.
5. Rouse, Rubber World 1992, 206, 25–29.
6. Baker, W. E.; Sharpe, J.; Rajalingam, P. Rubber Chem Technol 1993, 66, 664–677.
7. Bagheri, R.; Williams, M. A.; Pearson, R. A. Polym Eng Sci 1997, 37, 245–251.
8. Zanzotto, L.; Stastna, J.; Vacin, O. Appl Rheology 2000, 3, 134.
9. Mahlke, D. Kautsch Gummi Kunstst 1993, 11, 889.
10. Fuhrmann I.; Karger-Kocsis, J. Kautsch Gummi Kunstst 1999, 12, 836–841.
11. Buckley, D. J.; Berger, M.; Poller, D. J Polym Sci 1962, 56, 163–174.
12. Forte, R.; Leblanc, J. L. J Appl Polym Sci 1992, 45, 1473–1483.
13. Goodrich; Porter, Polym Eng Sci 1967, 7, 45.
14. Brandrup, J.; Immergut, E. H.; Grulke, E. A. Polymer Handbook, 4th ed.; 1999.
15. Crank, J. The Mathematics of Diffusion; Oxford Univ. Press, 1956.
16. Van Amerongen, G. J. Rubber Chem Technol 1964, 37, 1065–1152.
17. Crank, J. J Polym Sci 1953, 11, 151–168.
18. Southern, E. Use of Rubber in Engineering; MacLaren: London, 1967.
19. Lawandy, S. N.; Helaly, F. H. J Appl Polym Sci 1986, 32, 5279–5286.
20. Lawandy, S. N.; Wassef, M. T. J Appl Polym Sci 1990, 40, 323–331.
21. Mazich, K. A.; Rossi. G.; Smith, C. A. Macromolecules 1992, 25, 6929–6933.
22. Unnikrishnan, G.; Thomas, S. Polymer 1994, 35, 5504.
23. Barrière, B.; Liebler, L. J Appl Polym Sci, Part B: Polym Phys 2003, 41, 166–182.
24. Southern, E.; Thomas, A. G. Rubber Chem Technol 1969, 42, 495.
25. Rossi, G.; Mazich, K. A. Phys Rev E 1993, 48, 1181.
26. Abu-Abdeen, M.; Abdel Ghani, S. A. J Appl Polym Sci 2001, 81, 3169.